The limitations of the actual experiments are best studied through a comparison with the ideal situation. A close approximation to the ideal experimental arrangement is shown in Fig. 7.4.4.1 as a series of phase-space diagrams. The characteristic radiation from a conventional X-ray tube is almost uniformly distributed over the solid angle of 2π, and the relative width of the $K\alpha_1$ or $K\alpha_2$ emission line is typically $\Delta\lambda/\lambda = 5 \times 10^{-4}$. The acceptance and emittance windows of a flat perfect crystal are given in Fig. 7.4.4.1(*b*). The angular acceptance of the crystal (Darwin width) is typically less than 10^{-4} rad, and, if the width of the slit s or that of the crystal is small enough, none of the $K\alpha_2$ distribution falls within the window. Therefore, it is sufficient to study the size and divergence distributions of the beam in the $\lambda(K\alpha_1)$ plane only, as shown in Fig. 7.4.4.1(*c*). The beam transmitted by the flat monochromator and a slit is shown as the hatched area, and the part reflected by a small crystal by the cross-hatched area. The reflectivity curve of the crystal is probed when the crystal is rotated. In this schematic case, almost 100% of the beam contributes to the signal. The typical reflection profile shown in Fig. 7.4.4.2 reveals the details of the crystallite distribution of the sample (Suortti, 1985). The broken curve shows the calculated profile of the same reflection if the incident beam from a mosaic crystal monochromator had been used (see below).

The window of acceptance of a flat mosaic crystal is determined by the width of the mosaic distribution, which may be 100 times larger than the Darwin width of the reflection in

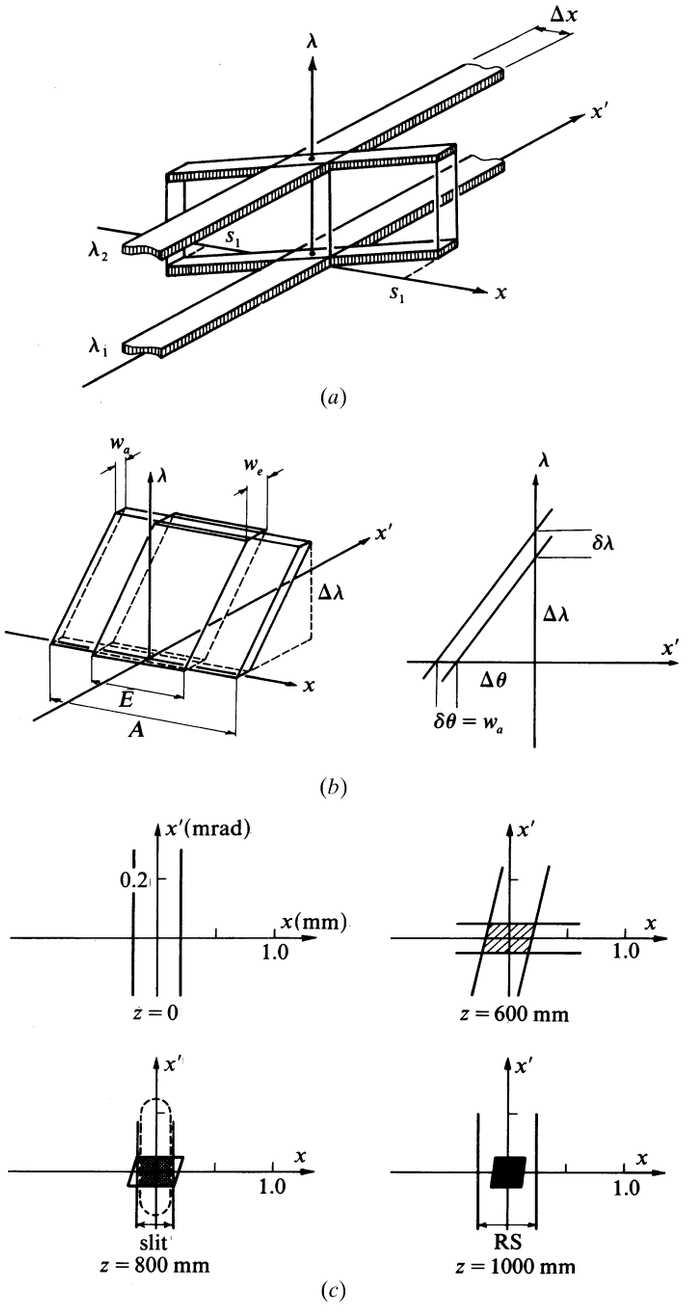

Fig. 7.4.4.1. Equatorial phase-space diagrams for a conventional X-ray source and parallel-beam geometry; x is the size and $x' = \mathrm{d}x/\mathrm{d}z$ the divergence of the X-rays. (*a*) Radiation distributions for two wavelengths, λ_1 and λ_2, at the source of width Δx, and downstream at a slit of width $\pm s_1$. (*b*) Acceptance and emittance windows of a flat perfect crystal, where the phase-space volume remains constant, $Aw_a\Delta\lambda = Ew_e\Delta\lambda$, and the (x', λ) section shows the reflection of a polychromatic beam (Laue diffraction). (*c*) Distributions for one wavelength at the source, flat perfect-crystal monochromator, sample (marked with the broken line), and the receiving slit (RS); z is the distance from the source.

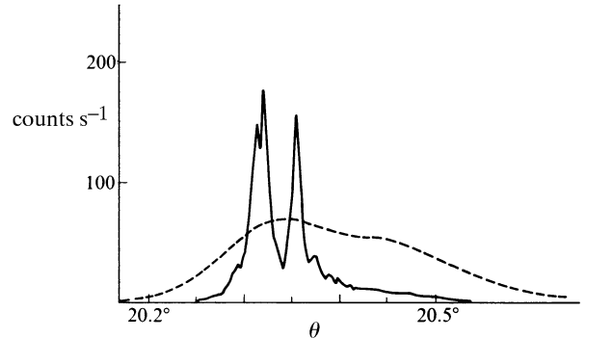

Fig. 7.4.4.2. Reflection 400 of LiH measured with a parallel beam of Mo $K\alpha_1$ radiation (solid curve). The broken curve shows the reflection as convoluted by a Gaussian instrumention function of $2\sigma = 0.1^\circ$ and $\theta(\alpha_2) - \theta(\alpha_1) = 0.13^\circ$, which values are comparable with those in Fig. 7.4.4.4.

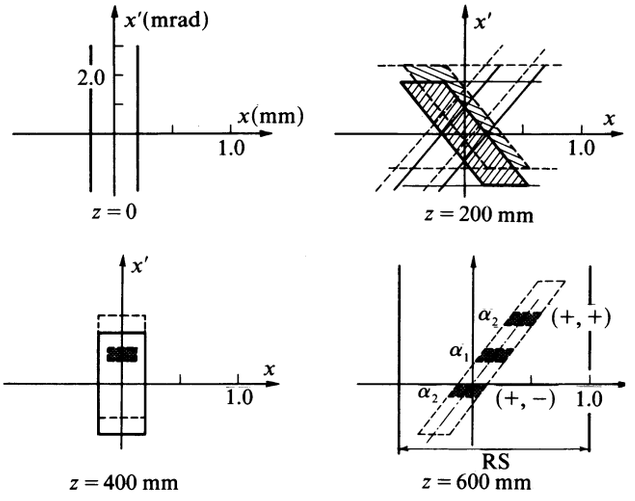

Fig. 7.4.4.3. Equatorial phase-space diagrams for two wavelengths, λ_1 (solid lines) and λ_2 (broken lines), projected on the plane $\lambda = \lambda_1$. The monochromator at $z = 200$ mm is a flat mosaic crystal, and a small sample is located at $z = 400$ mm, as shown by the shaded area. The reflected beams at the receiving slit are shown for the $(+, +)$ and $(+, -)$ configurations of the monochromator and the sample.

references